Vibrational Circular Dichroism Studies of the A-to-B Conformational Transition in DNA†

Lijiang Wang and Timothy A. Keiderling*

Department of Chemistry, University of Illinois at Chicago, Box 4348, Chicago, Illinois 60680

Received March 24, 1992; Revised Manuscript Received July 7, 1992

ABSTRACT: The vibrational circular dichroism (VCD) spectra of several natural DNAs as well as tRNA, poly(dG-dC)·poly(dG-dC), and poly(dA-dT)·poly(dA-dT) are reported for the base deformation modes in the IR region from 1700 to 1550 cm^{-1} for the polymers in D_2O as well as in high alcohol dehydrating conditions. Spectra of both the B- and A-forms were identified. The A-form DNA VCD, not previously reported, has characteristics that can be found in the VCD spectra of RNAs as would be expected from the similarity of their structures. The VCD is sequence-dependent. Under the dehydrating conditions studied, poly(dA-dT)poly(dA-dT), poly(dA)·poly(dT), and a high-A-T fraction natural DNA had a different bandshape from the other DNAs, which was similar to that of poly(rA)·poly(rU). Poly(dG-dC)·poly(dG-dC) did not form an A-form in high-alcohol conditions but instead had a VCD spectrum much like that of its high-salt-induced Z-form. Qualitative differences seen experimentally between A- and B-form DNA VCD were suggested by the differences in the coupled oscillator VCD calculated for the two forms.

Conformational studies of nucleic acids have involved use of a number of spectroscopic techniques (X-ray, NMR, IR, Raman, UV, CD, fluorescence, light scattering, etc.), chemical correlation, and computer modeling based on the known stereochemistry of the component parts [see Saenger (1984) and references cited therein]. Of these, electronic circular dichroism (ECD) in the UV has been widely used as a tool to monitor structural changes and the character of the resultant DNA or RNA conformations due to its high sensitivity to the nature of the secondary structure (Johnson, 1985). We have shown that circular dichroism measurements on RNA and DNAs are also possible in the infrared portion of the spectrum, which are there termed vibrational circular dichroism (VCD) (Annamalai & Keiderling, 1987; Yang & Keiderling, 1992; Keiderling et al., 1989). Diem and co-workers have also reported VCD of synthetic DNAs and have monitored their B- and Z-form conformations (Gulotta et al., 1989; Zhong et al., 1990). VCD measurements combine the structural sensitivity of optical activity with the resolution and localized excitation characteristics of vibrational spectroscopy. In particular, it is possible with VCD to independently probe the in-plane base deformation modes to reveal the interbase stereochemistry and stacking interactions, the phosphate P–O stretches to monitor the backbone stereochemistry, and various sugar modes to monitor the ribose conformation. Unlike the situation with ECD, the VCD of base modes for monophosphates is not detectable, so that the observed polymer VCD is a direct consequence of stacking interactions (Annamalai & Keiderling, 1987). Fundamentally, the relationship of VCD to ECD is one of enhanced resolution and localization of interactions. The cost for these advantages is somewhat more difficulty in doing the experiment in the infrared.

Single-stranded RNA samples gave rise to a bandshape which has been termed a positive VCD couplet [i.e., a first negative and then positive with decreasing frequency (Bayley, 1973)] typically centered over the most intense in-plane base deformation band which lies in the range of 1600–1700 cm^{-1} (Annamalai & Keiderling, 1987). In most cases, this band arises from the C=O stretching mode of the planar base. Dinucleotides and random copolymers have similar but weaker VCD, while duplex RNAs have similar patterns but are more intense. Intensity appears to correlate directly to helix stability as would be expected. Somewhat of an exception is the VCD of the duplex RNA, poly(rA)·poly(rU), which has a more complex, doubled pattern (Annamalai & Keiderling, 1987; Yang & Keiderling, 1992). This duplex also undergoes a two-to-three-strand conformational change with increase in temperature which has dramatic consequences in the VCD spectrum (Yang & Keiderling, 1992), indicating that VCD can easily detect triplex formation.

The generality in VCD bandshape found for simple polynucleotides has been attributed (Annamalai & Keiderling, 1987) to the regularity of the helix twist in these model systems. From a theoretical point of view, the relative stereochemistry of the bases, and hence of the dipole oscillators, is the same for all of these synthetic RNAs. This is probably the reason for the qualitative success of the coupled oscillator model in interpreting some DNA spectra (Zhong et al., 1990). The phosphate, PO_2^-, modes yield VCD signals that are more complex to interpret, but their intensities follow the same empirical intensity patterns with length and duplex formation as noted above for the C=O stretches (Yang & Keiderling, 1992).

The VCD spectra of poly(dG-dC) and related DNA oligomers which undergo a B- to Z-form transition have been subsequently reported for the base-stretching modes (Keiderling et al., 1989; Gulotta et al., 1989; Zhong et al., 1990; Wang et al., 1991). Distinctly different VCD spectra are measured for B- and Z-forms. Both types of spectra are dominated by a VCD couplet, but these are significantly shifted in frequency from each other and have opposite sign patterns which appear to be a consequence of the difference in the handedness of their respective polymeric backbones.

Having probed the B- to Z-form transition, the next obvious step in development of VCD as a structural tool for DNA studies is the characterization of the VCD changes occurring in the B- to A-form DNA transition and determination of its information content. Furthermore, it is important to determine

† This work was supported by a grant from the National Institutes of Health (GM 30147), and instrument purchases were aided by grants from the NSF, NIH, and University of Illinois.

0006-2960/92/0431-10265$03.00/0

if these observations based on synthetic DNA and RNA samples apply to natural DNAs with heterobase sequences. A-type and B-type DNAs are both right-handed helices, with the B-form being most common and the A-form favored under dehydrating conditions (Saenger, 1984; Vorlickova & Kypr, 1985). A-DNA has a 3′-endo sugar puckering conformation, its base pairs tilted by 20° with respect to the helix axis, and its axis dislocated by 4.7 Å into the major groove, which yields a deep and narrow major groove and a shallow minor groove. B-DNA double helices have the ribose conformation as 2′-endo, with the bases more nearly perpendicular to the helix axis and the grooves of comparable depth, although the major groove is wider than the minor groove. While the B-form is the predominant conformation in vivo, several experimental results have provided support for the idea that the A-type conformation of DNA could be biologically important (Wang, 1987; Frederick, 1984; Liquiers et al., 1990). Thus, it is important to characterize the A-form as well as to develop techniques of detecting these various conformations. Solution-phase A- and B-form DNA VCD spectra, measured in the C=O stretching and base deformation region, are presented in this paper. VCD spectra of natural DNAs as well as the more studied synthetic homopolymers are shown to be self-consistent and qualitatively interpretable.

MATERIALS AND METHODS

Except for calf thymus (lot 00544562) and chicken blood (lot 00424106) DNA obtained from Pharmacia, all the samples used in this study were purchased from Sigma, including *Clostridium perfringens* DNA (lot 28F4008), *Micrococcus lysodeikticus* DNA (lot 68F4017), poly(dA)·poly(dT) (lot 98F06561), poly(dA-dT)·poly(dA-dT) (lot 30H07121), and poly(dG-dC)·poly(dG-dC) (lot 99F02611), and used without further purification. Most of the DNA samples were deuterium-exchanged and redissolved in D_2O at a concentration of 15–40 mg/mL for B-form studies. To test the importance of prior deuterium exchange on the VCD, some samples were not exchanged first, but no significant difference was seen in the VCD. Trifluoroethanol (TFE)/D_2O solutions for A-form studies were made by adding TFE dropwise to concentrated DNA/D_2O solutions and stirring vigorously after each addition. These samples typically attained a final concentration of 2–4 mg/mL.

Alternatively, some samples were dissolved in sodium phosphate buffer (pD 7), as opposed to just D_2O, before addition of TFE. These typically precipitated at high TFE concentrations (70–80%). Thus, for the study of the B- to A-form transition, it was necessary to make the most of the measurements under nonbuffered conditions at apparent initial pHs in D_2O of ~5.5–7.7. There was one exception; it was possible to obtain A-form calf thymus DNA in an 85% TFE buffer solution to a final concentration of 0.67 mM $Na_{3/2}H_{3/2}PO_4$. It was found that the VCD spectra of calf thymus DNA both with and without buffer are essentially the same, which demonstrates that these nonbuffered DNA samples are sufficiently stable for VCD study on the time scale required.

All the VCD spectra reported here were measured with the dispersive VCD instrument constructed at UIC and described in detail in the literature (Keiderling, 1981, 1990). The instrumental conditions used for specific spectra are noted in the respective figure captions. In most cases, the spectra were collected with ~10-cm^{-1} resolution and 10-s time constant and are the average of four scans. Samples were placed in a cell composed of two CaF_2 windows separated by Teflon spacers of either 50 μm (D_2O) or 150–250 μm (TFE) in thickness depending on the solvent. Due to the relatively low (for VCD spectroscopy) DNA concentrations possible in the TFE/D_2O solutions, long path length and high sensitivity were required in order to obtain reasonable spectra. This consequently gave rise to somewhat low signal-to-noise ratio (S/N) VCD spectra. On the other hand, the low surface tension and relatively high vapor pressure of the alcohol solution prevent our use of longer path lengths with these cells. All VCD spectra reported herein were measured at room temperature since the B–A conformational transition has been shown to be temperature-independent under our experimental conditions (Ivanov et al., 1985).

For purposes of comparison, ECD spectra were obtained with a JASCO J-600 spectropolarimeter under continuous N_2 purge. Samples for ECD were made up at ~0.2–0.6 mg/mL concentration in D_2O and placed in a 1-mm path-length quartz cell. Spectra were measured from 180 to 300 nm. FTIR spectra of some of the VCD samples were measured with a Digilab FTS-60 instrument as a check of the dispersive result. All analyses of the VCD spectra were done using the absorbance spectra generated on the dispersive instrument under conditions identical to those used for VCD.

For the dehydration experiments, O-deuterated 1,1,1-trifluoroethanol was prepared from commercial TFE (Aldrich, AP). Metallic Na was added to a 1:8 mixture of TFE and D_2O to adjust the pH to ~8.5. After sitting at room temperature overnight, the mixture was distilled, and the TFE fraction was dried over $MgSO_4$ (Fisher) and then redistilled (70.0 ± 0.2 °C).

Since the magnitude of the observed VCD is proportional to the absorbance, normalization with respect to the absorbance is necessary in order to compare spectra obtained with various samples of poorly defined concentration and/or path length which consequently have absorbance bands of differing intensity. Since the DNA IR spectra have complex bandshapes due to the overlap of several transitions, a wavenumber range was chosen over which it is reasonable to assume that the total integrated absorbance intensity will be approximately constant in different DNAs and RNAs. After base-line correction, the area under the absorbance band for each sample was determined by integration using SpectraCalc software (Galactic Industries, Inc.). These integrated spectral areas from the dispersive measurements were arbitrarily normalized to an absorbance–frequency area of 30 cm^{-1} for plotting, and the same scaling factor was then used to normalize the VCD plots. Actual absorbances of the samples used in measuring the VCD were small, 0.06–0.2, a condition made possible by the relatively large rotational strengths of the DNA transitions.

RESULTS

Natural DNAs. The VCD and absorption spectra obtained at room temperature of the B-form natural DNA from chicken blood and calf thymus that we have studied here are effectively the same as reported earlier in preliminary communications (Keiderling et al., 1989; Wang et al., 1991). In Figure 1, the base deformation VCD for calf thymus DNA is illustrated as a dashed line for B-form and as a solid line for A-form. We have done several tests to explore the stability of these spectra with varying conditions. No detectable change was seen in the spectra of the same sample taken over a 2-day period. Similarly, no difference in VCD was seen, except for decreased S/N, for a sample measured with 4 times less concentration. All of these D_2O- or buffer-based DNA VCD spectra have a dominant positive VCD couplet with zero crossing at ~1685

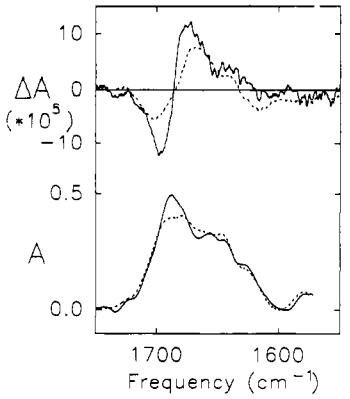

FIGURE 1: Comparison of A-form and B-form VCD spectra for the base deformation modes of calf thymus (- - -) B-form, 14 mg/mL, D_2O, 0.1-mm path length. (—) A-form, 3.5 mg/mL, 85% TFE/D_2O, 0.2-mm path length.

cm^{-1} centered over the highest energy intense base deformation absorption band. To lower energy at ~1640 cm^{-1}, these B-form natural DNAs have a positive VCD shoulder that falls below the second main absorption feature at ~1650 cm^{-1}. For some samples, the VCD seems to be broad and negative at and below 1600 cm^{-1}.

The B- to A-form conformational transition can be induced in DNA by lowering the level of hydration. In solution, such changes can be induced by decreasing the activity of water by addition of alcohol to the DNA solution (Sprecher et al., 1979; Ivanov et al., 1974; Brahms et al., 1982; Charney et al., 1991). We chose to use O-deuterated TFE for this purpose in order to improve the IR transparency of the resulting solution which made practical an increase in path length as compared to D_2O solutions. Consequently, it was possible to study solutions of lower DNA concentrations under high TFE concentration.

Adding TFE to an aqueous calf thymus DNA solution resulted in little difference in either the IR or the VCD bandshape over the range of 0–50% TFE added. Some differences became apparent at TFE concentrations over 70%, and the final, stable spectrum was attained at 85% added TFE (as illustrated by the solid line spectrum for calf thymus DNA in Figure 1). The same sort of VCD changes were seen for chicken blood DNA at 85% TFE. The spectral changes are consistent with a conformational transition having taken place during the last stages of the process. ECD spectra (in the UV from 200 to 300 nm) of such high-percentage TFE samples showed an increase in positive ECD at 265 nm and development of a strong negative ECD at 210 nm (Figure 2) which is consistent with the A-form DNA ECD bandshape reported previously (Sprecher et al., 1979) and confirms the formation of A-form DNA in the transition observed in our samples. The A-form DNA VCD observed is actually quite similar to that of B-form DNA, but the couplet is sharper and significantly more intense, as is the 1687-cm^{-1} IR absorption. On a relative scale, both techniques, VCD and ECD, have similar magnitude changes for the B-to-A transition.

The two natural DNAs discussed above happen to have very similar base compositions of ~44% G-C base pairs. DNA from *M. Lysodeikticus* contains ~72% G-C pairs. As seen in Figure 3, the evidence for its transition from B- to A-form DNA at high alcohol concentration was the same with VCD and IR as was seen for the other, lower G-C content DNAs, namely, a small frequency shift of the main feature at ~1684 cm^{-1} to higher energy and an increase of intensity in both VCD and absorbance spectra. ECD spectra of a series of TFE/D_2O solutions of *M. lysodeikticus* DNA showed that

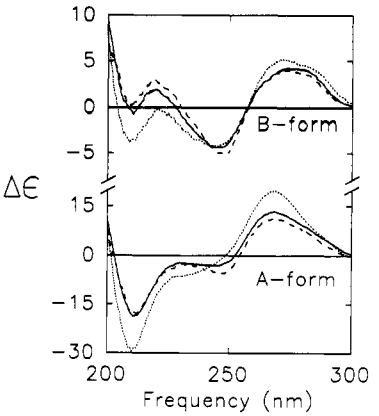

FIGURE 2: Comparison of ECD spectra for A-form and B-form DNA of (—) calf thymus (A-form, 0.51 mg/mL, 85% TFE/D_2O, 0.51 mg/mL, 1.0-mm path length; B-form, 0.57 mg/mL, D_2O, 1.0-mm path length), (···) *M. lysodeikticus* (A-form, 0.61 mg/mL, 80% TFE/H_2O, 1.0-mm path length; B-form, 0.53 mg/mL, H_2O, 1.0-mm path length), and (- - -) *C. perfringens* (A-form, 0.18 mg/mL, 80% TFE/H_2O, 1.0-mm path length; B-form, 0.53 mg/mL, H_2O, 1.0-mm path length).

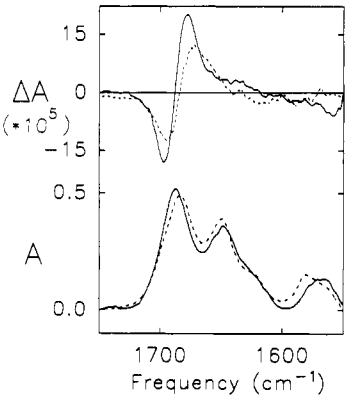

FIGURE 3: Comparison of A-form and B-form VCD spectra for the base deformation modes of *M. lysodeikticus* DNA. (- - -) B-form, 20 mg/mL, D_2O, 0.1-mm path length. (—) A-form, 3.5 mg/mL, 80% TFE/D_2O, 0.2-mm path length.

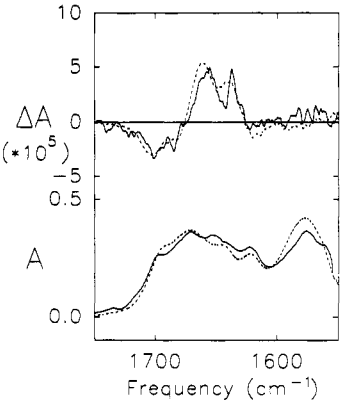

FIGURE 4: Comparison of A-form and B-form VCD spectra for the base deformation modes of *C. perfringens* DNA. (- - -) B-form, 36.7 mg/mL, D_2O, 0.05-mm path length. (—) A-form, 3.1 mg/mL, 80% TFE/D_2O, 0.2-mm path length.

a characteristic A-form DNA spectrum was found at 80% TFE (Figure 2, dotted line).

DNA from *C. perfringens*, consisting of only 26% G-C, yields a VCD spectrum different from those presented in Figures 1 and 3 for both its A-form and its B-form. As shown in Figure 4, the A-form, obtained at 80% TFE, has a much smaller change from the B-form result than seen in the previously discussed natural DNAs. By comparison with the

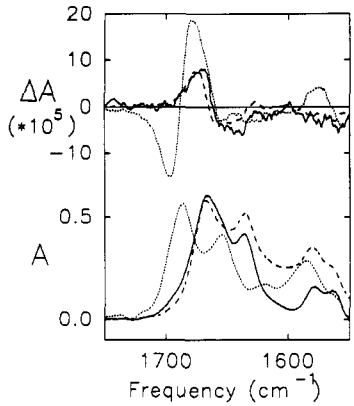

FIGURE 5: Comparison of the VCD spectra of the base deformation modes of B-form and Z-form poly(dG-dC)·poly(dG-dC). (···) B-form, 0.1 M NaCl/D_2O, 44 mg/mL, 0.05-mm path length. (- - -) Z-form, 4.7 M NaCl, 30 mg/mL, 0.025-mm path length. (—) Z-form, 80% TFE/D_2O, 3 mg/mL, 0.25-mm path length.

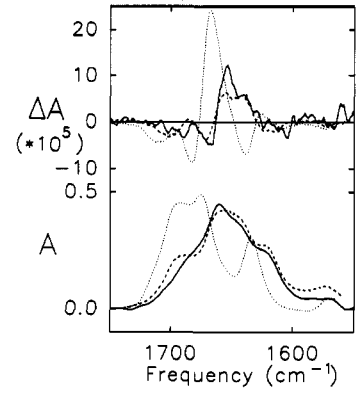

FIGURE 6: Comparison of the VCD spectra of the base deformation modes of poly(rA)·poly(rU) and the A-form and B-form of poly(dA-dT)·poly(dA-dT). (···) Poly(rA)·poly(rU), 45 mg/mL, 0.1 M NaCl/D_2O, 0.025-mm path length. (- - -) B-form of poly(dA-dT)·poly(dA-dT), 28 mg/mL, D_2O, 0.05-mm path length. (—) A-form of poly(dA-dT)·poly(dA-dT), 80% TFE/D_2O, 2 mg/mL, 0.25-mm path length.

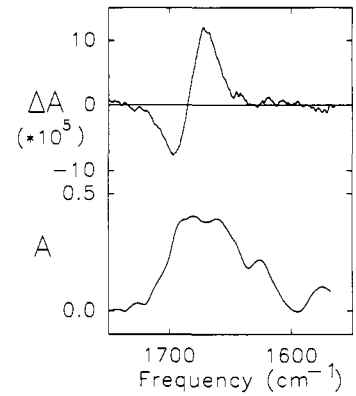

FIGURE 7: VCD spectra of the base deformation modes of tRNA from yeast: 0.1 M NaCl/D_2O, 40 mg/mL, 0.025-mm path length.

VCD of the high-G-C DNAs, the negative feature in this spectrum has two broad lobes. All the VCD peaks sharpened (solid line) as the DNA changed from B- to A-form, but the two positive bands are shifted, in this case, to *lower* energy by ~4–6 cm^{-1}. That this small VCD change represents the B-to-A transition for *C. perfringens* is demonstrated by the corresponding ECD spectra in Figure 2 (dashed line). In summary, on transforming from B- to A-form, the natural DNAs studied gave small relative bandshape but significant intensity changes in their VCD spectra with the exception of *C. perfringens* DNA which has a much higher A-T content yielding VCD of a different spectral shape and less magnitude change.

Synthetic DNAs. Comparison of the natural DNA spectra presented above to those of synthetic DNAs is also useful. The VCD of B-form poly(dG-dC) (Figure 5, dotted line) is similar to that of the natural B-form DNAs in Figures 1 and 3 even though a significant difference in the absorption bandshape is evident. As compared to the natural A-form DNAs, poly(dG-dC) does not undergo a B- to A-form transition in 80% TFE/D_2O but instead gives rise to a VCD spectrum that is characteristic of a left-handed Z-form DNA (Figure 5, solid line). The inverted VCD sign pattern (to what is roughly analogous to a negative couplet) and the lowered frequency of the zero crossing of the negative couplet with respect to the positive couplet zero crossing for the right-handed A- and B-forms are dramatic bandshape changes leaving no doubt as to the type of transition occurring. The result in Figure 5 is consistent with our earlier VCD studies of B- to Z-form transitions in DNA stimulated by increased salt concentration (dashed line; Keiderling et al., 1989; Yang et al., unpublished results) and is in reasonable agreement (other than magnitude, which is dependent on counterion and state of aggregation) with the published results of Diem's laboratory (Gulotta et al., 1989). This VCD frequency shift follows the shift of the absorbance maximum from 1690 to 1660 cm^{-1} on Z-formation. The Z-form VCD spectra for high-salt and high-TFE poly(dG-dC) are not exactly the same, having a 5-cm^{-1} difference in zero crossing which is probably attributable to solvent.

Similar high TFE concentration studies were made using poly(dA-dT)·poly(dA-dT) and resulted in spectra (solid line, Figure 6) with only small changes from the D_2O result (dashed line) much as seen in the *C. perfringens* natural DNA example (Figure 4). Runs of consecutive A·T pairs are known to stabilize B-DNA relative to A-DNA, but the existence of A-form poly(dA-dT)·poly(dA-dT) has been supported by a number of experiments (Vorlickova et al., 1985; Loprete & Hartman, 1990; Ivanov et al., 1985). Consistent with this, our ECD spectra showed a very different result for poly(dA-dT)·poly(dA-dT) in an 80% TFE solution as compared to that for aqueous poly(dA-dT)·poly(dA-dT). A characteristic negative band was observed at about 215 nm which may imply that some A-form DNA was formed under these experimental conditions. Our VCD spectra indicate that the B- to A-form transition that occurs under the conditions used for the poly(dA-dT)·poly(dA-dT) VCD is characterized by a frequency down-shift of the weak negative feature at ~1700 cm^{-1} and an intensity increase of the couplet at ~1670 cm^{-1}. The absorbance spectrum also develops a significant shoulder at 1700 cm^{-1} under high-TFE conditions.

RNA Comparison. Since the A-form of DNA is quite similar to the conformation expected for duplex RNA, one can compare the VCD of natural DNAs to that of natural, partially "A-form-like" tRNA, illustrated in Figure 7. When normalized to the area of its absorbance band, the VCD of tRNA was smaller than that of the high-G-C A-form DNAs illustrated in Figures 1 and 3. This is consistent with the absorption bandshape of tRNA which does not exhibit the relatively sharp, higher energy peak at 1685 cm^{-1} normally seen in those DNAs. Such a broader shape probably arises from the heterogeneous structure of tRNA which encompasses loops and mismatches as well as duplex stems.

A second comparison can be made between the VCD of synthetic RNA and that of A-form DNA. Our previously

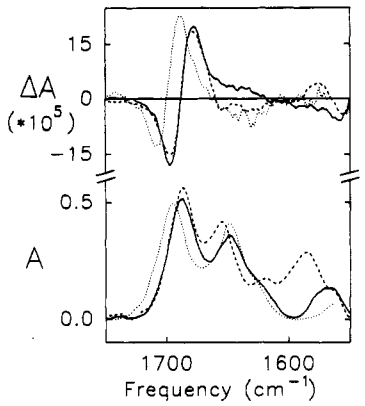

FIGURE 8: Comparison of VCD spectra for the base deformation modes of B-form poly(dG-dC)·poly(dG-dC), A-form *M. lysodeikticus*, and A-form poly(rI)·poly(rC). (···) Poly(rI)·poly(rC), 0.1 M NaCl/D_2O, 30 mg/mL, 0.05-mm path length. (- - -) Poly(dG-dC)·poly(dG-dC), 0.1 M NaCl/D_2O, 44 mg/mL, 0.05-mm path length. (—) *M. lysodeikticus*, 3.5 mg/mL, 80% TFE/D_2O, 0.2-mm path length.

reported VCD of single-strand and duplex RNAs show the highest energy sharp, intense transition is also correlated with a positive VCD couplet. The comparison can be most clearly seen in Figure 8, where the VCD for poly(rI)·poly(rC) is shown as the dotted line spectrum (Annamalai & Keiderling, 1987) and the high-G-C content, *M. lysodeikticus* DNA is shown as a solid line. The highest energy transition in each is sharp and intense and gives rise to an intense positive couplet in both. The magnitude of this poly(rI)·poly(rC) VCD signal is virtually the same as that seen for the high-G-C content A-form DNAs in Figures 1 and 3, but it is shifted up in frequency by 10 cm^{-1}. By comparison, the VCD of B-form poly(dG-dC) (dashed line) is somewhat weaker than that of A-form *M. lysodeikticus* (solid line) and of its RNA analogue (dotted line, Figure 8). The main VCD feature in each case corresponds to the highest frequency absorbance maxima. This is in contrast to the poly(rA)·poly(rU) or poly(dA-dT)·poly(dA-dT) situation where the main VCD couplet corresponds to the second maximum. Poly(dA-dT)·poly(dA-dT) VCD spectra resemble that of poly(rA)·poly(rU), but are significantly broader and much weaker (40%) than the RNA spectrum (Annamalai & Keiderling, 1987; Yang & Keiderling, 1992) as shown in Figure 6. Zhong et al. (1990) have previously reported poly(dA-dT)·poly(dA-dT) and poly(dA-dT) VCD in D_2O which have very similar shapes and are in qualitative agreement with our results.

DISCUSSION

General Empirical Observations. It is clear from our data that VCD can be used to detect a conformational transition from the B- to A-form of DNA. These can be detected in a variety of DNAs, natural and synthetic, all of which can be interpreted in a consistent manner. However, since the fundamental relative bandshape does not change, this B-to-A spectral transition is not nearly so dramatic as that seen in going from the B- to Z-form (Keiderling et al., 1989; Gulotta et al., 1989; Zhong et al., 1990; Wang et al., 1991). It can be concluded from our experimental results that the conformational transition from B- to A-form DNA leads to the sharpening and intensifying of the VCD band in the carbonyl stretching region, making it more similar to the RNA results for comparable systems. However, this spectral characteristic of the B-to-A transition is not independent of sequence. We see quite a different response to dehydration in the VCD spectra for DNAs rich in G-C content as opposed to those rich in A-T content while in ECD there is a much smaller difference in bandshape (Figure 2). This base dependence was extreme for the synthetic DNAs tested since our dG-dC sample underwent a B- to Z-form transition instead of the desired B- to A-form. Since the VCD spectrum reflects coupling of local oscillators, particularly the C=O stretches, which differ for each base, it should not be so surprising that the VCD is sensitive to sequence. On the other hand, the ECD spectrum senses coupling of the π-electron systems which have substantial similarities among the bases and, thus, is less sensitive.

However, it is possible to reach a reasonable qualitative understanding of the nature of the A-form VCD observed through comparison to our previously reported RNA results (Yang & Keiderling, 1992; Annamalai & Keiderling, 1987). The natural DNA A-form VCD for high-G-C content DNAs is about the same magnitude as that for the poly(rI)·poly(rC) VCD, which is reasonable due to the similarity of their structures. When different heterogeneous structures are compared, calf thymus and chicken blood DNAs have the same shaped VCD spectrum as does tRNA but are higher in intensity due to the fraction of bases in the tRNA loops which presumably contribute little to the VCD intensity but do increase the absorbance. The A-form natural DNA VCD is more intense than the single-strand RNA VCD (Annamalai & Keiderling, 1987) due to the effect of base pairing on the relative stability of the helix with respect to the coil form. It is smaller than the VCD of the synthetic duplex RNA due to the heterogeneity of the sequence. The similarities of VCD spectra between calf thymus DNA, chicken blood DNA, and tRNA in terms of the bandshapes and magnitudes of the VCD bands follow from their similar G-C contents (~44% for both DNAs and ~52% for yeast tRNA). The consistency of A-form DNA with RNA results is further evidence that the VCD comes from coupling of the base modes through stacking and is independent of the nature of the ribose.

The sequence dependence of DNA VCD is the reason that the VCD of *M. lysodeikticus* DNA (72% G-C) resembles that of poly(dG-dC)·poly(dG·dC), while the VCD of *C. perfringens* DNA (26% G-C) is more like that of poly(dA-dT)·poly(dA-dT) and poly(dA)·poly(dT). This fact led us to attempt to synthesize the VCD spectra of natural DNAs from the appropriate linear combinations of the poly(dG-dC) and poly(dA-dT) VCD. The G-C-dominant *M. lysodeikticus* DNA has a synthesized VCD very similar to that observed experimentally, but the others were less well predicted. This error may result from unique interactions between the different bases so that if the DNA in question were structured more like a block copolymer, this simple spectral simulation would work well. Its failure is indicative of the heterogeneity of the sequence, but this is a relatively small effect. In principle, VCD thus provides a method of discriminating between types of DNA sequences, from both a base content and a sequence perspective.

The poly(dA-dT)·poly(dA-dT) and poly(dA)·poly(dT) DNA VCD patterns [Figure 6 and Zhong et al. (1990)] resemble that of poly(rA)·poly(rU) and are quite different from the G-C-dominant DNAs and RNAs. This probably arises from the interactions of the two C=O groups on the T base and suggests that the interaction between A's is somewhat independent of that between T's based on our previous analysis of the poly(rA)·poly(rU) results (Yang & Keiderling, 1992).

Poly(dG-dC)·poly(dG-dC) (Figure 5) gives rise to a left-handed helical Z-form in 80–83% TFE/D_2O which shows a reversed VCD sign pattern with respect to the results from

the right-handed A- and B-forms. This characteristic Z-form VCD is well established (Keiderling et al., 1989; Gulotta et al., 1989), and the dependence of the VCD sign pattern on the helicity of the oscillators is well understood from theoretical (Zhong et al., 1990; Birke et al., 1992) and experimental points of view (Dukor & Keiderling, 1991; Gulotta et al., 1991). This result is consistent with the results of Brahms et al. (1982), who saw Z-form ECD in high TFE concentrations (from 60% to 85%). Hall and Maestre (1984) found a Z′-form ECD for 85% ethanol solutions, but Riazance et al. (1985) and Ivanov and Minyat (1981) apparently mistakenly interpreted similar ECD observations for poly(dG-dC)·poly(dG-dC) in 80–84% TFE solution as due to A-form DNA. VCD makes a clear distinction here between Z-form and A-form so that there is no doubt that, at these high concentrations in 80% TFE, the dominant conformation is Z-form in our poly(dG-dC) samples. This distinction arises from the dominance for DNA VCD of exciton coupling. A parallel is seen in the relative ease of predictability of far-UV ECD spectra which are also dominated by exciton coupling (Williams et al., 1986). It is the near-UV data, normally used to characterize Z- and A-forms, that lead to confusion not present with VCD. Harder and Johnson (1990) have reported a careful comparison of the ECD spectra for Z- and Z′-forms as a function of divalent ion concentration. The ECD of our samples is closer to their Z-form spectra, so that divalents, though probably present at low levels, are not a serious problem for the DNA concentrations used in VCD.

Computational Studies. While we have established some qualitative relationships of the spectral characteristics of the B- to A-form DNA transitions with the properties of synthetic and natural RNAs, we cannot yet explain why the transition from an arrangement of bases in the center of the helix and oriented normal to its axis (B-form) gives less intense (or broader) VCD than an arrangement with the bases spread out from the axis and tilted with respect to it (A-form). A possible means of understanding this difference might be available from a comparison of the results of coupled oscillator calculations (Holzwarth & Chabay, 1972; Gulotta et al., 1989) for the two structures. Hopefully, such calculations would indicate if dipolar coupling changes could account for the differences in A- and B-form spectra. Diem and co-workers have formulated a dipole coupling formalism of use for modeling the pairwise interaction of several degenerate dipole oscillators in an oligomeric form (Gulotta et al., 1989). For the base deformation modes in nucleic acids, this model poses a reasonable level of approximation. These local modes, being coupled by multiple bonds through two sugars and a phosphate, are relatively mechanically isolated and, due to the planar structure of the bases, are locally achiral. Initial reports from Diem's laboratory have indicated success in calculationally reproducing the qualitative B-form DNA VCD bandshape for poly(dG-dC)·poly(dG-dC) and related oligomers (Zhong et al., 1990). However, the VCD magnitudes calculated with this model are still a problem, making it unlikely to be capable of quantitatively explaining the difference we have seen in the A- and B-form DNA VCD spectra. Nonetheless, we have carried out such calculations with the motivation that it would be interesting to learn the *relative magnitudes predicted for the A- and B-form VCD* even if both were inaccurate on an absolute scale.

Initially, we attempted to reproduce the published coupled oscillator calculated VCD for the poly(dG-dC)·poly(dG-dC) carbonyl stretches as represented by a series of oligomers. However, the formula for D_k should involve a double sum over the coupled dipoles, which would make the off-diagonal contribution in the computations reported by Zhong et al. (1990) undercalculated by a factor of 2. This correction has some effect on the relative intensity of the components of the calculated exciton band. Using the standard B-form geometry for DNA incorporated into the Quanta software (Polygen), the coupled oscillator VCD was calculated using this correction of the Gullotta et al. (1989) formulas and a transition dipole strength of $D = 0.33$ D^2 which was derived from the band parameters given by Zhong et al. (1990) of $\epsilon = 950$ L·(mol·cm)$^{-1}$ and a width of 20 cm^{-1} (HWHH).

One potential problem with these B-form calculations is determination of the proper dipole strength and use of it to calculate the frequency dispersion for the exciton band. Use of a smaller D value caused the absorbance splittings to collapse so that the C=O vibrations gave rise to just a broadened band rather than a split transition while use of a much larger value results in too much spread between exciton components. The VCD bandshape, however, retains most of its characteristic features over such variation, but the main feature shifts to lower frequency and loses its intensity if calculated with a lower D value. Thus, a real question remains of how can one develop a reasonable estimate of the VCD when the absorbance prediction is so ambiguous. The stability of the bandshape for the VCD as computed with various D values led us to continue calculations for the A-form despite this problem, but the variation of the magnitude suggested that one should be skeptical with regard to the quantitative aspects of such calculations.

In our A-form calculations, as was also found by Zhong et al. (1990) for the B-form, very different VCD bandshapes result for the two dimers G-C and C-G which is primarily a result of very different dispersions for the transition frequencies, but the same bandshape is calculated for the trimers C-G-C and G-C-G. (In that B-form report, the labels for G and C were apparently reversed.) For the decamer $(dC\text{-}dG)_5$, a pattern consistent with the experimental result was calculated having the main positive VCD couplet associated with the highest energy absorption band. However, the splitting of the main absorbance peaks appears to be overestimated by nearly a factor of 2 when we use the D value noted above, as optimized for the B-form. Hence, the fundamental problem of quantification with this model remains and seems centered on estimating the exciton splitting using dipole coupling.

Our original goal was to use these calculations to pinpoint some qualitative difference in the B- and A-form VCD. Since in the coupled oscillator picture the A-form has a much larger dipole splitting than the B-form, the A-form absorbance maximum appears at a higher energy than the B-form, echoing the frequency shift seen experimentally in the B- to A-form transition for high-G-C content DNAs. In the coupled oscillator calculated VCD, both forms give rise to positive couplets centered on the highest frequency component of the absorption, with the A-form VCD intensity being stronger, again qualitatively reproducing the experimental result. Overall, one can conclude that the high-G-C content DNA VCD is qualitatively well reflected in the DCO calculations.

One can also calculate the same sort of spectra for the A-T oligomers, but due to there being two non equivalent C=O groups on the T base and none on the A base, the method does not work satisfactorily. The apparent agreement found by Zhong et al. (1990) for a model of poly(dA)·poly(dT) with coupled oscillator calculations for that structure appears to be fortuitous in that it was based on a misassignment of the

C=O group involved in the hydrogen bonding. A proper assignment results in a band shape totally unlike the experimental one obtained for the poly(dA)·poly(dT) model. Given the lack of qualitative agreement of theory with experiment for this structure, it seems pointless to discuss our computational results for the A-T system further. We must rely at present on the qualitative trends seen in the G-C system.

CONCLUSIONS

The effect of the B-to-A transition on the VCD of the base deformation (primarily C=O and C-N stretching) region in the IR is less dramatic than the B-to-Z VCD change but is significant. The VCD pattern of A-form natural DNA is very much like that of poly(rI)·poly(rC) and natural tRNA. However, VCD of just the in-plane base modes is apparently not sufficient for critically delimiting the more subtle changes seen in a B-to-A transition. On the other hand, VCD does evidence a fairly strong dependence on the sequence or, more precisely, on the relative G-C content.

The calculational approach of Diem and co-workers does not seem to be very general, but this may derive from its dependence as originally formulated on the dipole interaction of only C=O modes. Work by Cianciosi et al. (1991) has shown that inclusion of other oscillators can aid the development of a qualitative representation of the VCD of small molecules where the coupled oscillator effect can be important. Perhaps future study of the PO_2^- modes characteristic of the backbone conformation would provide a more informative means of monitoring the structural changes involved in the B–A transition. While we cannot measure VCD for the PO_2^- modes for DNAs in TFE solutions, we have measured B- and Z-form PO_2^- VCD spectra for DNA and for A-like RNA (Wang et al., unpublished results). Development of reliable methods of determining film VCD for these species would also help in delineation of the characteristics of these lower frequency transitions.

ACKNOWLEDGMENT

We gratefully acknowledge Prof. Max Diem for sharing preprints of his work in this area before publication, Dr. A. Annamalai and Mr. Ligang Yang for measurement of some preliminary spectra, and Mr. Petr Bour for identifying some difficulties with the coupled oscillator calculations.

REFERENCES

Annamalai A., & Keiderling, T. A. (1987) *J. Am. Chem. Soc. 109*, 3125–3132.
Bayley, P. M. (1973) *Prog. Biophys. Mol. Biol. 27*, 1–76.
Birke, S. S., Agbaje, I., & Diem, M. (1992) *Biochemistry 31*, 450–455.
Brahms, S., Vergne, J., Brahms, J. G., Di Capua, E., Bucher, Ph., & Koller, Th. (1982) *J. Mol. Biol. 162*, 473–493.
Charney, E., Chen, H.-H., & Rau, D. C. (1991) *J. Biomol. Struct. Dyn. 9(2)*, 353–362.
Cianciosi, S. J., Ragunathan, N., Freedman, T. B., Nafie, L. A., Lewis, D. K., Glenar, D. A., & Baldwin, J. E. (1991) *J. Am. Chem. Soc. 113*, 1864–1866.
Dukor, R. K., & Keiderling, T. A. (1991) *Biopolymers 31*, 1747–1761.
Frederick, C. A., Grable, J., Melia, M., Jen-Jacobsen, L., Samudzi, C., Wang, W. C., Itakura, K., Greene, P., Boyer, H., & Rosenberg, J. M. (1984) *Nature 309*, 327–331.
Gulotta, M., Goss, D. J., & Diem, M. (1989) *Biopolymers 28*, 2047–2058.
Gulotta, M., Zhong, W., Goss, D. J., Votavova, & Diem, M. (1991) in *Spectroscopy of Biological Molecules* (Hester, R. E., & Girling, J., Eds.) pp 135–136, Royal Society of Chemistry, Cambridge, U.K.
Hall, K. B., & Maestre, M. F. (1984) *Biopolymers 23*, 2127–2139.
Harder, M. E., & Johnson, W. C., Jr. (1990) *Nucleic Acids Res. 18*, 2141–2148.
Holzwarth, G., & Chabay, I. (1972) *J. Chem. Phys. 57*, 1632–1635.
Ivanov, V. I., & Minyat, E. E. (1981) *Nucleic Acids Res. 9(18)*, 4783–4798.
Ivanov, V. I., Minchenkova, L. E., Minyat, E. E., Frank-Kamenetskii, M. D., & Schyolkina, A. K. (1974) *J. Mol. Biol. 87*, 817–833.
Ivanov, V. I., Krylov, D. Y., & Minyat, E. E. (1985) *J. Biomol. Struct. Dyn. 3(1)*, 43–55.
Johnson, W. C., Jr. (1985) *Methods Biochem. Anal. 31*, 61–163.
Keiderling, T. A. (1981) *Appl. Spectrosc. Rev. 17*, 189–226.
Keiderling, T. A. (1990) in *Practical Fourier Transform Infrared Spectroscopy Industrial and Laboratory Analyses* (Ferraro, J. R., & Krishnan, K., Eds.) pp 203–284, Academic Press, San Diego.
Keiderling, T. A., Yasui, S. C., Pancoska, P., Dukor, R. K., & Yang, L. (1989) *Proc. SPIE—Int. Soc. Opt. Eng. 1057*, 7–14.
Liquiers, J., Taillandier, E., Peticolas, W. L., & Thomas, G. A. (1990) *J. Biomol. Struct. Dyn. 8(2)*, 295–302.
Loprete, D. M., & Hartman, K. A. (1990) *Biopolymers 30*, 753–761.
Pilet, J., Blicharski, J., & Brahms, J. (1975) *Biochemistry 4*, 1869–1876.
Riazance, J. H., Baase, W. A., Johnson, W. C., Jr., Hall, K., Cruz, P., & Tinnoco, I., Jr. (1985) *Nucleic Acids Res. 13(13)*, 4983–4989.
Rich, A., Nordheim, A., & Wang, A. H.-J. (1984) *Annu. Rev. Biochem. 53*, 791–846.
Saenger, W. (1984) in *Principles of Nucleic Acid Structure* (Cantor, C. R., Ed.) pp 253–282, Springer-Verlag, New York.
Sprecher, C. A., Baase, W. A., & Johnson, W. C., Jr. (1979) *Biopolymers 18*, 1009–1019.
Vorlickova, M., & Kypr, J. (1985) *J. Biomol. Struct. Dyn. 3(1)*, 67–83.
Vorlickova, M., Seslacek, P., Kypr, J., & Sponar, J. (1982) *Nucleic Acids Res. 10(21)*, 6969–6070.
Wang, A. H.-J. (1987) *Nucleic Acids and Molecular Biology* (Eckstein, F., & Lilley, D. M. J., Eds.) Vol. 1, pp 53–69, Springer-Verlag, Berlin and Heidelberg.
Wang, L., Yang, L., & Keiderling, T. A. (1991) in *Spectroscopy of Biological Molecules* (Hester, R. E., & Girling, J., Eds.) pp 137–138, Royal Society of Chemistry, Cambridge, U.K.
Williams, A. L., Cheong, C., Tinoco, I., Jr., & Clark, L. B. (1986) *Nucleic Acids Res. 14*, 6649–6659.
Yang, L., & Keiderling, T. A. (1992) *Biopolymers* (in press).
Zhong, W., Gulotta, M., Goss, D. J., & Diem, M. (1990) *Biochemistry 29*, 7485–7491.